

FLAT-FACED LEADING-EDGE EFFECTS ON SHOCK-DETACHMENT DISTANCE IN HYPERSONIC WEDGE FLOW

Wilson F. N. Santos

wilson@lcp.inpe.br

Combustion and Propulsion Laboratory, National Institute for Space Research
Cachoeira Paulista, SP 12630-000 Brazil

***Abstract.** This work deals with a numerical study on truncated wedges situated in a rarefied hypersonic flow. The work is motivated by the interest in investigating the blunting effects on the shock wave structure. The primary aim of this paper is to examine the sensitivity of the shock standoff distance and shock wave thickness to shape variations of such flat-faced leading edges. In addition, to provide a critical analysis on maximum allowable geometric bluntness, dictated by either handling or manufacturing requirements, resulting on reduced departures from ideal aerodynamic performance of the original sharp leading edge. The impact of the blunting effects on the shock wave structure is investigated, through the Direct Simulation Monte Carlo (DSMC) method, by a model that classifies the molecules in three distinct classes, i.e., “undisturbed freestream”, “reflected from the boundary” and “scattered”, i.e., molecules that had been indirectly affected by the presence of the leading edge. As expected, it was found that the shock standoff distance and the shock thickness increased by increasing the flat-face thickness. The analysis also showed a blunt-body shock wave structure for a leading edge with thickness of just one freestream mean free path.*

***Keywords:** Hypersonic flow, Rarefied Flow, DSMC, Shock standoff distance, Wedge.*

1. INTRODUCTION

Hypersonic configurations are generally characterized by slender bodies and sharp leading edges in order to achieve good aerodynamic properties like high lift and low drag. Certain configurations, such as waveriders (Nonweiler, 1959), usually exhibit very high lift-to-drag ratios when inviscid flow is assumed. Waveriders are designed analytically with infinity sharp leading edges for shock wave attachment. As the shock wave is attached to the leading edge of the vehicle, the upper and lower surfaces of the vehicle can be designed separately. Moreover, the attached shock wave may prevent spillage of higher-pressure airflow from the lower side of the vehicle to the upper side, resulting in a high-pressure differential and enhanced lift.

Usually, it is extremely difficult to construct a perfectly sharp leading edge. Any manufacturing error may result in a significant deviation from the initial design contour. Furthermore, sharp edges are difficult to maintain because they are easily damaged. In addition to that, as heat transfer in the stagnation region increases inversely with the square root of the leading edge radius, high heating is associated with sharp edges. Therefore, for practical hypersonic configurations, leading edges are blunted for heat transfer, manufacturing, and handling concerns. Because blunt leading edge promotes shock standoff, practical leading edges will have shock detachment, making leading-edge blunting a major concern in the design and prediction of flowfields over hypersonic waveriders.

Many experimental and theoretical works (Vidal & Bartz, 1966; McCroskey et al., 1967; Chow & Eilers, 1968; Vidal & Bartz, 1969; Allègre et al., 1969; Klemm & Giddens, 1977) with wedges have been carried out with “aerodynamically sharp” leading edges. Nevertheless, a critical study providing information on the maximum allowable edge thickness for a given flow pattern has not received considerable attention. On the other hand, the flowfield properties upstream the leading edge of a body are affected by molecules reflected from the the edge region, and the degree of the effect is in part conditioned by the edge geometry.

In this connection, Santos (2002, 2004) has investigated the leading edge thickness effect on the flowfield structure of truncated wedge at zero angle of attack in a rarefied hypersonic flow. The thickness effect was examined for a range of Knudsen number, based on the thickness of the frontal face, covering from the transitional flow regime to the free molecular flow regime. Some significant differences between sharp and blunt leading edges was found on the flowfield structure. The analysis showed that the upstream effects have different influence on velocity, density, pressure and temperature along the stagnation streamline ahead of the leading edges. The flowfield approached the free molecular flow in the vicinity of the frontal face of the wedge as the leading edge thickness was of the order of one hundredth of the freestream mean free path.

In an effort to obtain further insight into the nature of the flowfield structure of truncated wedge under hypersonic transitional flow conditions, Santos (2003) extended the analysis presented by Santos (2002) by performing a parametric study on these shapes with a great deal of emphasis placed on the compressibility effects. The primary aim was to assess the sensitivity of the pressure, skin friction, heat transfer and drag coefficients to variations on the freestream Mach number. It was observed that large effects on the flowfield structure and on the surface quantities due to leading edge thickness are possible even with models whose leading edges are generally considered as being aerodynamically sharp.

Based on recent interest in hypersonic waveriders for high-altitude/low-density applications (Anderson, 1990; Potter & Rockaway, 1994; Rault, 1994; Graves & Argrow, 2001), the present account extends the analysis presented by Santos (2004) by examining computationally the shock wave structure over these truncated wedges. The primary goal is to assess the sensitivity of the shock standoff distance and of the shock wave thickness to variations on the

thickness of the leading edge. In addition, to provide a critical analysis on a maximum allowable geometric bluntness, dictated by either handling or manufacturing requirements, resulting on reduced departures from ideal aerodynamic performance of the vehicle. Thus allowing the blunted leading edge to more closely represent the original sharp leading edge flowfield.

The present study is focused on the low-density region in the upper atmosphere, where the non-equilibrium conditions are such that traditional CFD calculations are inappropriate to yield accurate results. In such a circumstance, the Direct Simulation Monte Carlo (DSMC) method will be employed to calculate the rarefied hypersonic two-dimensional flow on the leading edge shapes.

2. LEADING-EDGE GEOMETRY DEFINITION

The truncated wedges analyzed in this work are modeled by assuming a sharp leading edge of half angle θ with a circular cylinder of radius R inscribed tangent to this sharp leading edge. The truncated wedges are also tangent to both the sharp leading edge and the cylinder. It was assumed a leading edge half angle of 10 deg, a circular cylinder diameter of 10^{-2} m and frontal surface thickness t/λ_∞ of 0, 0.01, 0.1 and 1, where λ_∞ is the freestream molecular mean free path. Figure 1 illustrates schematically this construction. The common body height H and the body length L are obtained in a straightforward manner. It was assumed that the leading edges are infinitely long but only the length L is considered, since the wake region behind the leading edges is not of interest in this investigation.

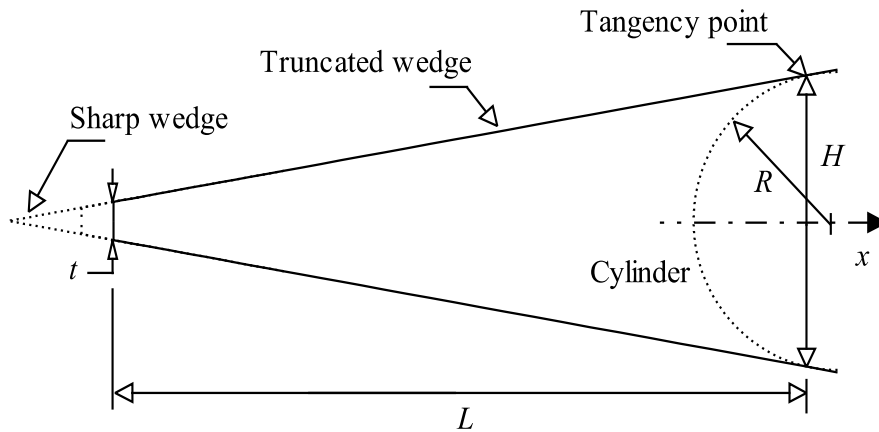


Figure 1: Drawing illustrating the leading edge geometry.

3. COMPUTATIONAL METHOD

The Direct Simulation Monte Carlo (DSMC) method, pioneered by Bird (1994), has proved to be the most efficient technique for computing flowfields in which rarefaction effects play a significant role.

In the DSMC method, the gas is modeled at the microscopic level by using simulated particles, which each one represents a very large number of physical molecules or atoms. These representative molecules are tracked as they move, collide and undergo boundary interactions in simulated physical space. The molecular motion, which is considered to be deterministic, and the intermolecular collisions, which are considered to be stochastic, are uncoupled over the small time step used to advance the simulation and computed sequentially. The simulation is always calculated as unsteady flow. However, a steady flow solution is obtained as the large

time state of the simulation.

The molecular collisions are modeled using the variable hard sphere (VHS) molecular model (Bird, 1981) and the no time counter (NTC) collision sampling technique (Bird, 1989). The VHS model assumes that the cross section of a molecule changes with the collision energy according to some power law. The exponent is calculated by matching the viscosity of the simulated gas to that of its real counterpart. In addition, the VHS model assumes an isotropic scattering in the center of mass frame of reference.

Simulations are performed using a non-reacting gas model consisting of two chemical species, N_2 and O_2 . For polyatomic particles, transfer of energy to and from the internal modes has to be considered. In this way, energy exchanges between the translational and internal modes are considered. The energy exchange between kinetic and internal modes is controlled by the Borgnakke-Larsen statistical model (Borgnakke & Larsen, 1975). For a given collision, the probabilities are designated by the inverse of the relaxation numbers, which correspond to the number of collisions necessary, on average, for a molecule to relax. In this study, the relaxation numbers of 5 and 50 were used for the rotation and vibration, respectively.

For the numerical treatment of the problem, the flowfield around the leading edges is divided into an arbitrary number of regions, which are subdivided into computational cells. The cells are further subdivided into subcells, two subcells/cell in each coordinate direction. The cell provides a convenient reference for the sampling of the macroscopic gas properties, while the collision partners are selected from the same subcell for the establishment of the collision rate.

The computational domain used for the calculation is made large enough so that body disturbances do not reach the upstream and side boundaries, where freestream conditions are specified. A schematic view of the computational domain is depicted in Fig. 2.

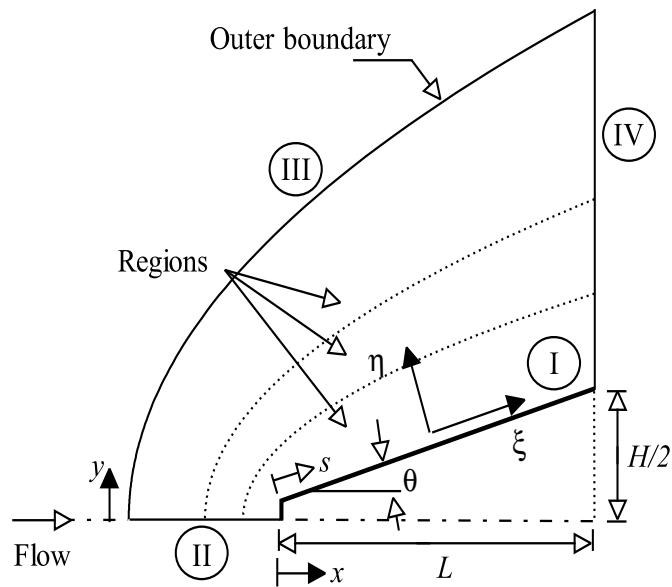


Figure 2: Schematic view of the computational domain.

Side I is defined by the body surface. Diffuse reflection with complete thermal accommodation is the condition applied to this side. In a diffuse reflection, the molecules are reflected equally in all directions, and the final velocity of the molecules is randomly assigned according to a half-range Maxwellian distribution determined by the wall temperature. Advantage of the flow symmetry is taken into account, and molecular simulation is applied to one-half of a full

configuration. Thus, side II is a plane of symmetry, where all flow gradients normal to the plane are zero. At the molecular level, this plane is equivalent to a specular reflecting boundary. Side III is the freestream side through which simulated molecules enter and exit. Finally, the flow at the downstream outflow boundary, side IV, is predominantly supersonic and vacuum condition is specified (Guo & Liaw, 2001). At this boundary, simulated molecules can only exit.

The numerical accuracy in DSMC method depends on the cell size chosen, on the time step as well as on the number of particles per computational cell. In the DSMC algorithm, the linear dimensions of the cells should be small in comparison with the scale length of the macroscopic flow gradients normal to streamwise directions, which means that the cell dimensions should be of the order of or smaller than the local mean free path (Alexander et al., 1998, 2000). The time step should be chosen to be sufficiently small in comparison with the local mean collision time (Garcia & Wagner, 2000; Hadjiconstantinou, 2000). In general, the total simulation time, discretized into time steps, is identified with the physical time of the real flow. Finally, the number of simulated particles has to be large enough to make statistical correlations between particles insignificant.

These effects were investigated in order to determine the number of cells and the number of particles required to achieve grid independence solutions. Grid independence was tested by running the calculations with half and double the number of cells in ξ and η directions (see Fig. 2) compared to a standard grid. Solutions (not shown) were near identical for all grids used and were considered fully grid independent. A discussion of these effects on the aerodynamic surface quantities is described in details in Santos (2004).

4. FREESTREAM AND FLOW CONDITIONS

The flow conditions represent those experienced by a spacecraft at an altitude of 70 km. This altitude is associated with the transitional regime, which is characterized by the overall Knudsen number of the order of or larger than 10^{-2} .

The freestream flow conditions used for the numerical simulation of flow past the leading edges are those given by Santos (2002, 2004) and summarized in Table 1, and the gas properties (Bird, 1994) are shown in Table 2.

Referring to Tables 1 and 2, T_∞ , p_∞ , ρ_∞ , μ_∞ , n_∞ , and λ_∞ stand respectively for the temperature, pressure, density, viscosity, number density and the molecular mean free path, and X , m , d and ω account respectively for the mass fraction, molecular mass, molecular diameter and the viscosity index.

The freestream velocity V_∞ is assumed to be constant at 3.5 km/s, which corresponds to a freestream Mach number M_∞ of 12. The leading edge surface has a constant wall temperature T_w of 880 K for all cases considered. This wall temperature represents the temperature usually attained in an actively-cooled metallic leading edge. Furthermore, these flow conditions may represent the top end of an ascending hypersonic trajectory as well as be representative of a maneuvering reentry vehicle.

The overall Knudsen number Kn is defined as the ratio of the molecular mean free path λ in the freestream gas to a characteristic dimension of the flowfield. In the present study, the characteristic dimension was defined as being the thickness t of the frontal surface. For the thicknesses investigated, t/λ_∞ of 0, 0.01, 0.1 and 1, the overall Knudsen numbers correspond to Kn_t of ∞ , 100, 10 and 1, respectively. Finally, the Reynolds number Re_t covers the range from 0.193 to 19.3, based on conditions in the undisturbed stream with leading edge thickness t as the characteristic length.

Table 1: Freestream flow conditions

Altitude (km)	T_∞ (K)	p_∞ (N/m ²)	ρ_∞ (kg/m ³)	μ_∞ (Ns/m ²)	n_∞ (m ⁻³)	λ_∞ (m)
70	220.0	5.582	8.753×10^{-5}	1.455×10^{-2}	1.8209×10^{21}	9.03×10^{-4}

Table 2: Gas properties

	X	m (kg)	d (m)	ω
O_2	0.237	5.312×10^{-26}	4.01×10^{-10}	0.77
N_2	0.763	4.650×10^{-26}	4.11×10^{-10}	0.74

5. COMPUTATIONAL PROCEDURE

The problem of predicting the thickness, shape and location of detached shock waves has been stimulated by the necessity for blunt noses and leading edges configurations designed for hypersonic flight in order to cope with the aerodynamic heating. In addition, the ability to predict the thickness, shape and location of shock waves is of primary importance in analysis of aerodynamic interference. Furthermore, the knowledge of the shock wave displacement is especially important in a waverider geometry (Nonweiler, 1959), since this hypersonic configuration usually relies on shock wave attachment at the leading edge to achieve its high lift-to-drag ratio at high-lift coefficient.

In this present account, the shock wave structure, defined by thickness and detachment of the shock wave, is predicted by employing a procedure based on the physics of the particles. In this respect, the flow is assumed to consist of three distinct classes of molecules; those molecules from the freestream that have not been affected by the presence of the leading edge are denoted as class I molecules; those molecules that, at some time in their past history, have struck and been reflected from the body surface are denoted as class II molecules; and finally, those molecules that have been indirectly affected by the presence of the body are defined as class III molecules. Figure 3 illustrates the definition for the molecular classes.

It is assumed that the class I molecule changes to class III molecule when it collides with class II or class III molecule. Class I or class III molecule is progressively transformed into class II molecule when it interacts with the body surface. Also, a class II molecule remains class II regardless of subsequent collisions and interactions. Hence, the transition from class I molecules to class III molecules may represent the shock wave, and the transition from class III to class II may define the boundary layer.

A typical distribution of class III molecules along the stagnation streamline for blunt leading edges is displayed in Fig. 4 along with the definition used to determine the thickness, displacement and shape of the shock wave. In this figure, X is the distance x along the stagnation streamline (see Fig. 2), normalized by the freestream mean free path λ_∞ , and f_{III} is the number of molecules for class III to the total amount of molecules inside each cell.

In a rarefied flow, the shock wave has a finite region that depends on the transport properties of the gas, and can no longer be considered as a discontinuity obeying the classical Rankine-Hugoniot relations. In this context, the shock standoff distance Δ is defined as being the dis-

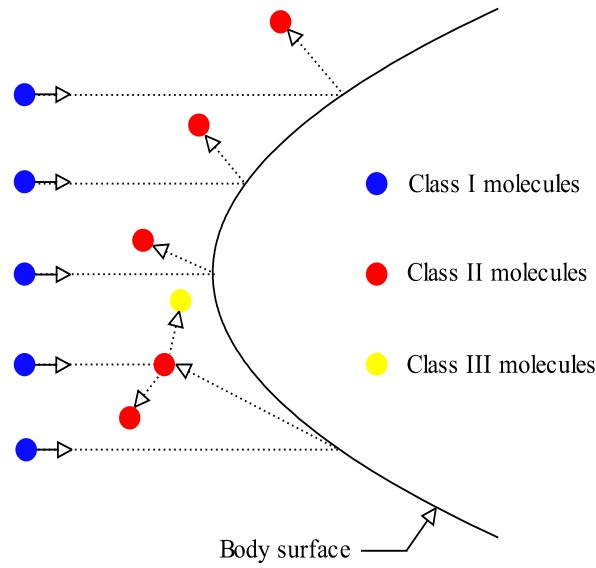


Figure 3: Drawing illustrating the classification of molecules.

tance between the shock wave center and the nose of the leading edge along the stagnation streamline. As shown in Fig. 4, the center of the shock wave is defined by the station that corresponds to the maximum value for f_{III} . The shock wave thickness δ is defined by the distance between the stations that correspond to the mean value for f_{III} . Finally, the shock wave “location” is determined by the coordinate points given by the maximum value in the f_{III} distribution along the lines departing from the body surface, i.e., η -direction as shown in Fig. 2.

The molecule classification that has been adopted here was first presented by Lubonski (1962) in order to study the hypervelocity Couette flow near the free molecule regime. Lubonski (1962) divided the gas into three classes of molecules: “freestream”, “reflected from the boundary” and “scattered”. Later, for the purpose of flow visualization, Bird (1969) applied the same scheme of classification by identifying the classes by colors: blue for class I, red for class II and yellow for class III molecules.

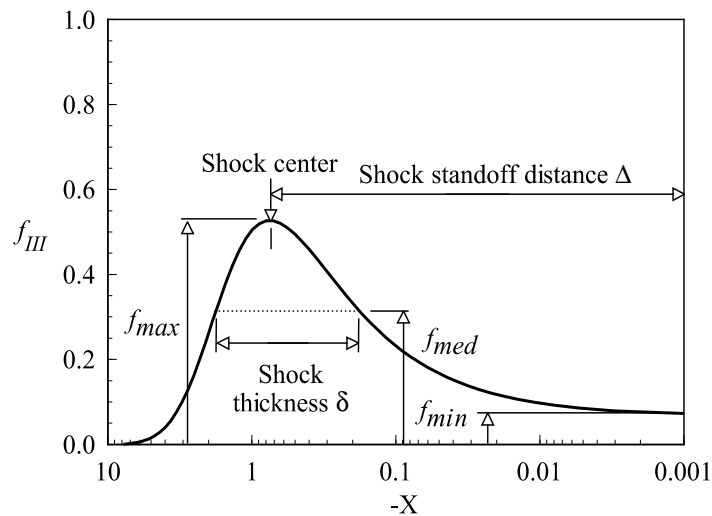


Figure 4: Drawing illustrating the shock wave structure.

6. COMPUTATIONAL RESULTS AND DISCUSSION

The purpose of this section is to discuss and to compare differences in the thickness and displacement of the shock wave due to variations on the leading edge thickness.

The distribution of molecules for the three classes along the stagnation streamline is illustrated from Figs. 5 to 8 for Knudsen number Kn_t of ∞ , 100, 10 and 1, respectively. These four cases correspond to t/λ_∞ of 0, 0.01, 0.1 and 1, respectively.

Referring to this set of figures, f_I , f_{II} and f_{III} are the ratio of the number of molecules for class I, II and III, respectively, to the total amount of molecules inside each cell along the stagnation streamline, X is the distance x along the stagnation streamline normalized by the freestream mean free path λ_∞ . Finally, the flow direction is from left to right as defined in Fig. 2.

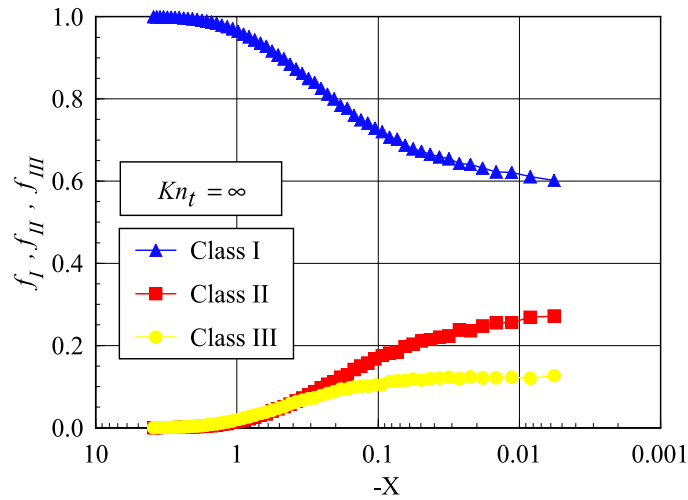


Figure 5: Distributions of molecules for classes I, II and III along the stagnation streamline for leading edge thickness t/λ_∞ of 0 that corresponds to Kn_t of ∞ .

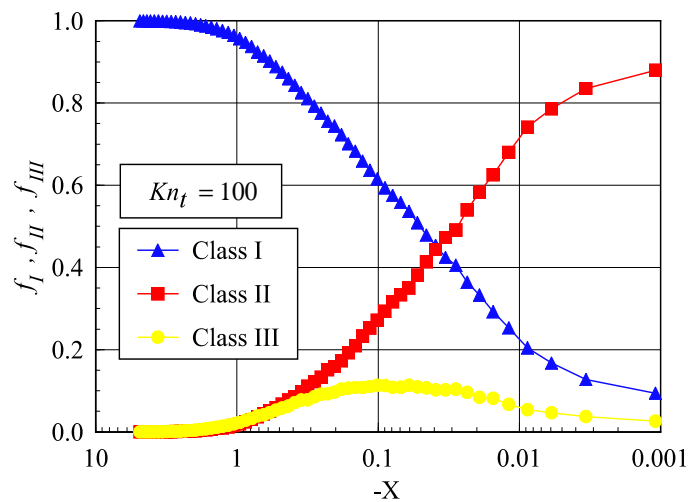


Figure 6: Distributions of molecules for classes I, II and III along the stagnation streamline for leading edge thickness t/λ_∞ of 0.01 that corresponds to Kn_t of 100.

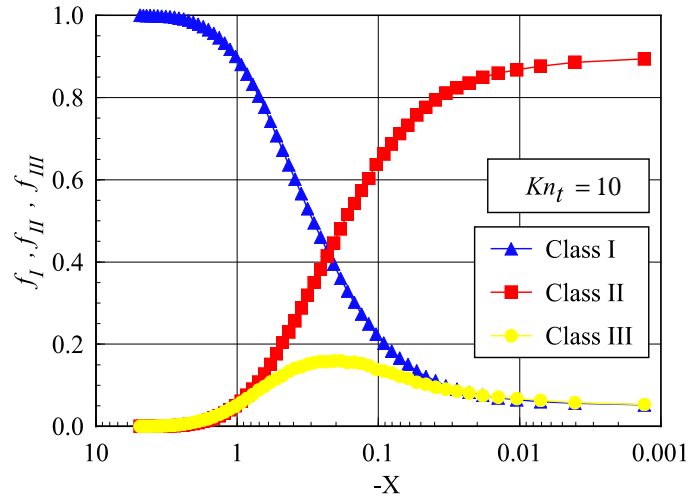


Figure 7: Distributions of molecules for classes I, II and III along the stagnation streamline for leading edge thickness t/λ_∞ of 0.1 that corresponds to Kn_t of 10.

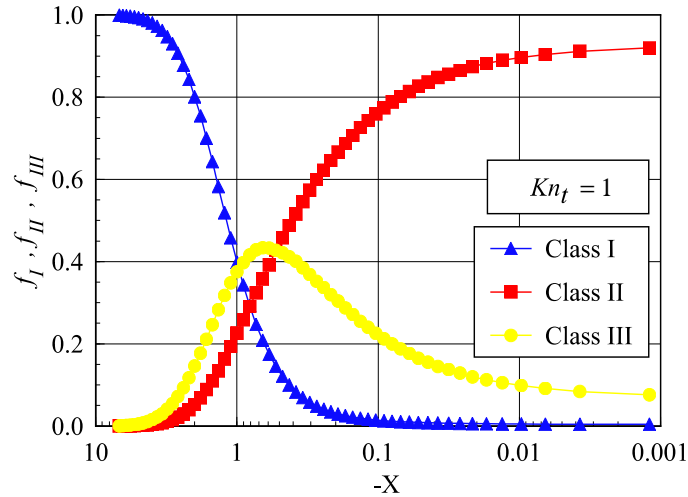


Figure 8: Distributions of molecules for classes I, II and III along the stagnation streamline for leading edge thickness t/λ_∞ of 1 that corresponds to Kn_t of 1.

Of great significance in these figures is the behavior of the molecules for sharp and blunt leading edges. It should be noticed that molecules from freestream, represented by class I molecules, collide with the nose of the leading edges for the cases with t/λ_∞ of 0, 0.01, 0.1, even after the establishment of the steady state. This is shown from Figs. 5 to 7, which represent sharp leading edge cases. In contrast, molecules from freestream do not reach the nose of the leading edge for the case t/λ_∞ of 1, as illustrated in Fig. 8, that represents a blunt leading edge. This is explained by the fact that density (Santos, 2004) increases much more for blunt (flat) leading edges in the stagnation region and reaches its maximum value in the stagnation point. In this connection, the buildup of particle density near the nose of the leading edge acts as a shield for the molecules coming from the undisturbed stream.

6.1 Shock Wave Standoff Distance

According to the definition shown in Fig. 4, the shock wave standoff distance Δ can be observed from Figs. 5 to 8 for the shapes shown. It is apparent from these results that there is a discrete shock standoff distance for the cases shown, except for the sharp leading edge case, $t/\lambda_\infty = 0$, where the maximum for f_{III} occurs in the stagnation point.

The calculated shock wave standoff distance Δ , normalized by the freestream mean free path λ_∞ , is tabulated in Table 3 for the cases investigated. As would be expected, the shock standoff distance increases with increasing the frontal surface thickness. As a reference, the shock wave standoff distance for the bluntest leading edge case, $Kn_t = 1$, is around 2.9 and 6.4 times larger than those for Kn_t of 10 and 100, respectively.

For comparison purpose, the round leading edge (circular cylinder), shown in Fig. 1, provides a shock detachment Δ/λ_∞ of 1.645 at the same flow conditions (Santos & Lewis, 2004). This value is about 17.2, 7.9 and 2.4 times larger than the cases corresponding to Kn_t of 100, 10 and 1, respectively. The results confirm the expectation that the shock standoff distance for sharp leading edge is smaller than that for blunt leading edge. In fact, the flat-faced leading edges (truncated wedge) behave as if they had a sharper profile than the representative round leading edge (circular cylinder).

It should be recognized that shock standoff distance becomes important in hypersonic vehicles such as waveriders, which depend on the leading edge shock attachment to achieve their high lift-to-drag ratio at high lift coefficient. Nonetheless, smaller shock detachment distance is associated with a higher heat load to the nose of the body. According to Santos (2002, 2004), the heat transfer coefficient $C_h (= 2q_w/\rho_\infty V_\infty^3)$ at the stagnation point for $t/\lambda_\infty = 0.01$ is 1.1 and 1.5 times larger than the heat transfer coefficient for the cases t/λ_∞ of 0.1 and 1, respectively, at the same conditions.

Table 3: Dimensionless shock wave standoff distance Δ/λ_∞ for the leading edges.

$t/\lambda_\infty = 0$ ($Kn_t = \infty$)	$t/\lambda_\infty = 0.01$ ($Kn_t = 100$)	$t/\lambda_\infty = 0.1$ ($Kn_t = 10$)	$t/\lambda_\infty = 1$ ($Kn_t = 1$)
0.0	0.096	0.209	0.614

6.2 Shock Wave Thickness

Based on the definition of the shock wave thickness shown in Fig. 4, the shock wave thickness δ along the stagnation streamline can be obtained from Figs. 5 to 8 for the leading edge shapes. As a result of the calculation, Table 4 tabulates the shock wave thickness δ , normalized by the freestream mean free path λ_∞ , for the cases investigated.

Table 4: Dimensionless shock wave thickness δ/λ_∞ for the leading edges.

$t/\lambda_\infty = 0$ ($Kn_t = \infty$)	$t/\lambda_\infty = 0.01$ ($Kn_t = 100$)	$t/\lambda_\infty = 0.1$ ($Kn_t = 10$)	$t/\lambda_\infty = 1$ ($Kn_t = 1$)
0.0	0.385	0.528	1.342

As a result of the simulation, the shock wave thickness for the bluntest leading edge case, $Kn_t = 1$, is around 3.5 and 2.5 times larger than those for Kn_t of 10 and 100, respectively.

In what follows, the round leading edge (circular cylinder) provides a much larger shock thickness, i.e., δ/λ_∞ , of 3.350 at the same flow conditions (Santos & Lewis, 2004). Compared to the truncated wedges, this value is about 8.7, 6.3 and 2.5 times larger than the cases corresponding to Kn_t of 100, 10 and 1, respectively.

7. CONCLUDING REMARKS

This study applies the Direct Simulation Monte Carlo method to investigate the shock wave structure for a family of flat-faced leading edges. The calculations have provided information concerning the nature of the shock wave detachment distance and shock wave thickness resulting from variations on the thickness of the frontal surface for the idealized situation of two-dimensional hypersonic rarefied flow. The emphasis of the investigation was to compare these flat-faced leading edges with a sharp leading edge (wedge) in order to determine the maximum allowable geometric bluntness resulting on reduced departures from ideal aerodynamic performance in terms of the shock wave standoff distance and shock wave thickness. The analysis showed that the shock wave structure was affected by changes on the thickness of the frontal surface. It was found that the shock wave standoff and the shock wave thickness increased by increasing the flat face for the conditions investigated.

REFERENCES

- Alexander, F. J., Garcia, A. L., & Alder, B. J., 1998. Cell Size Dependence of Transport Coefficient in Stochastic Particle Algorithms. *Physics of Fluids*, vol. 10, n. 6, pp. 1540–1542.
- Alexander, F. J., Garcia, A. L., & Alder, B. J., 2000. Erratum: Cell Size Dependence of Transport Coefficient in Stochastic Particle Algorithms. *Physics of Fluids*, vol. 12, n. 3, pp. 731–731.
- Allègre, J., Herpe, G. & Faulmann, D., 1969. Measurements of Pressure Distribution, Drag and Lift on Flat Plates and Wedges at Mach 8 in Rarefied Gas Flow. In Trilling, L., Wachman, H. Y., eds., *Proceedings of the 6th International Symposium on Rarefied Gas Dynamics*, Academic Press, New York, vol. I, pp. 465–482.
- Anderson, J. L., 1990. Tethered Aerothermodynamic Research for Hypersonic Waveriders. In *Proceedings of the 1st International Hypersonic Waverider Symposium*, Univ. of Maryland, College Park, MD, 1990.
- Bird, G. A., 1969. The Structure of Rarefied Gas Flows Past Simple Aerodynamic Shapes. *Journal of Fluid Mechanics*, vol. 36, n. 3, pp. 571–576.
- Bird, G. A., 1981. Monte Carlo Simulation in an Engineering Context. In Fisher, S. S., ed., *Progress in Astronautics and Aeronautics: Rarefied gas Dynamics*, vol. 74, part I, AIAA New York, pp. 239–255.
- Bird, G. A., 1989. Perception of Numerical Method in Rarefied Gasdynamics. In Muntz, E. P., Weaver, D. P. & Capbell, D. H., eds., *Rarefied Gas Dynamics: Theoretical and Computational Techniques*, Vol. 118, Progress in Astronautics and Aeronautics, AIAA, New York, pp. 374–395.
- Bird, G. A., 1994. *Molecular Gas Dynamics and the Direct Simulation of Gas Flows* Oxford University Press.

- Borgnakke, C. & Larsen, P. S., 1975. Statistical Collision Model for Monte Carlo Simulation of Polyatomic Gas Mixture. *Journal of Computational Physics*, vol. 18, n. 4, pp. 405–420.
- Chow, W. L., & Eilers, R. E., 1968. Hypersonic Low-Density Flow past Slender Wedges. *AIAA Journal*, vol. 6, n. 1, pp.177–179.
- Garcia, A. L., & Wagner, W., 2000. Time Step Truncation Error in Direct Simulation Monte Carlo. *Physics of Fluids*, vol. 12, n. 10, pp. 2621–2633.
- Graves, R. E. & Argrow, B. M., 2001. Aerodynamic Performance of an Osculating-Cones Waverider at High Altitudes. In *35th AIAA Thermophysics Conference*, AIAA Paper 2001-2960, Anaheim, CA.
- Guo, K., & Liaw, G. S., 2001. A Review: Boundary Conditions for the DSMC Method. In *Proceedings of the 35th AIAA Thermophysics Conference*, AIAA Paper 2001-2953, 11–14 Jun, Anaheim.
- Hadjiconstantinou, N. G., 2000. Analysis of Discretization in the Direct Simulation Monte Carlo. *Physics of Fluids*, vol. 12, n. 10, pp. 2634–2638.
- Klemm, F. J., & Giddens, D. P., 1977. A Numerical Solution to the Problem of Low-Density Hypersonic Wedge Flow. In Potter, J. L., ed., *Rarefied gas Dynamics: Progress in Astronautics and Aeronautics*, Vol. 51, part I, pp. 313–322.
- Lubonski, J., 1962. Hypersonic Plane Couette Flow Rarefied Gas. *Archiwum Mechaniki Stosowanej*, vol. 14, n. 3/4, pp. 553–560.
- McCroskey, W. J., Bogdonoff, S. M., & Genchi, A. P., 1967. Leading Edge Flow Studies of Sharp Bodies in Rarefied Hypersonic Flow. in Brundin, C. L., ed., *Rarefied Gas Dynamics*, Academic Press, New York, pp. 1047–1066.
- Nonweiler, T. R. F., 1959. Aerodynamic Problems of Manned Space Vehicles. *Journal of the Royal Aeronautical Society*, vol. 63, Sept, pp. 521–528.
- Potter, J. L., & Rockaway, J. K., 1994. Aerodynamic Optimization for Hypersonic Flight at Very High Altitudes. In Shizgal, B. D. & Weaver, D. P., eds, *Rarefied Gas Dynamics: Space Science and Engineering*, Vol. 160, Progress in Astronautics and Aeronautics, AIAA New York, pp. 296–307.
- Rault, D. F. G., 1994. Aerodynamic Characteristics of a Hypersonic Viscous Optimized Waverider at High Altitude. *Journal of Spacecraft and Rockets*, vol. 31, n. 5, pp. 719–727.
- Santos, W. F. N., 2002. Truncated Leading Edge Effects on Flowfield Structure of a Wedge in Low Density Hypersonic Flight Speed. In *Proceedings of the 9th Brazilian Congress of Engineering and Thermal Sciences, ENCIT2002*, 11–18 Oct 2002, Caxambu, MG, Brazil.
- Santos, W. F. N., 2003. Compressibility Effects on Flowfield Structure of Truncated Wedges in Low-Density Hypersonic Flow. In *Proceedings of the 17th International Congress of Mechanical Engineering, COBEM2003*, 10–14 Nov 2003, São Paulo, SP, Brazil.
- Santos, W. F. N., 2004. Flat-Faced Leading-Edge Effects in Low-Density Hypersonic Wedge Flow. *Journal of Spacecraft and Rockets*, (to appear, in press).
- Santos, W. F. N., & Lewis, J. M., 2004. Aerothermodynamic Performance Analysis of Hypersonic Flow on Power Law Leading Edges. *Journal of Spacecraft and Rockets*, (to appear, in press).

Vidal, R. J., & Bartz, J. A., 1966. Experimental Studies of Low-Density Effects in Hypersonic Wedge Flows. In Leeuw, J. H., ed., *Rarefied Gas Dynamics*, Academic Press, New York, vol. I, pp. 467–486.

Vidal, R. J., & Bartz, J. A., 1969. Surface Measurements on Sharp Flat Plates and Wedges in Low-Density Hypersonic Flow. *AIAA Journal*, vol. 7, n. 6, pp. 1099–1109.